REPORT DOCUMENTATION PAGE

Form Approved OMB No. 0704-0188

1. REPORT DATE *(DD-MM-YYYY)*	**2. REPORT TYPE**	**3. DATES COVERED** *(From - To)*
21-01-2008	Conference Paper	21 January 2008

4. TITLE AND SUBTITLE

Ultra Compact Polymer and Silicon Modulator Design Based on Photonic Crystal Ring Resonators

5a. CONTRACT NUMBER
IN-HOUSE

5b. GRANT NUMBER

5c. PROGRAM ELEMENT NUMBER
61102F

6. AUTHOR(S)

Richard A. Soref[2], Zexuan Qiang[1], Weidong Zhou1[1] and Zhenqiang Ma[3]

5d. PROJECT NUMBER
2305

5e. TASK NUMBER
HC

5f. WORK UNIT NUMBER
01

7. PERFORMING ORGANIZATION NAME(S) AND ADDRESS(ES)

[1] Dept. of Engineering, NanoFAB Center, University of Texas at Arlington, TX 76019; [2] Optoelectronic Technology Branch, (AFRL/RYHC), 80 Scott Drive, Hanscom AFB, MA 01731-2909; [3]Dept. of Electrical and Computer Engineering, University of Wisconsin-Madison, WI 53706

8. PERFORMING ORGANIZATION REPORT

9. SPONSORING / MONITORING AGENCY NAME(S) AND ADDRESS(ES)

Electromagnetics Technology Division Source Code: 437890
Sensors Directorate
Air Force Research Laboratory
80 Scott Drive
Hanscom AFB MA 01731-2909

10. SPONSOR/MONITOR'S ACRONYM(S)
AFRL/RYHC

11. SPONSOR/MONITOR'S REPORT NUMBER(S)
AFRL-RY-HS-TP-2008-0004

12. DISTRIBUTION / AVAILABILITY STATEMENT

DISTRIBUTION A: APPROVED FOR PUBLIC RELEASE; DISTRIBUTION UNLIMITED.

13. SUPPLEMENTARY NOTES

The U. S. Government is joint author of this work and has the right to use, modify, reproduce, release, perform, display or discuss the work. Published in Proceedings of the SPIE, Volume 6896, 12 February 2008. Clearance number, ESC-08-0014

14. ABSTRACT

Ultra-small silicon-based photonic-crystal ring resonators (PCRRs), both passive and active, will be key contributors to the emerging low-power nanophotonic technology. We have modeled and simulated the diameter-dependent loss, Q, and FSR of such PCRRs and find a 0.02 dB "intrinsic" loss that is independent of diameter, unlike the ~1/D loss of micro-strip resonators. Close to 100% drop efficiency at the drop channel of 1557.5nm was obtained by design with a high spectral selectivity of Q greater than 1319 in the single-ring PCRR-based add-drop filters with ring radius of 1.2 □m. Ultra-compact polymer modulators were proposed and simulated, based on the hybrid integration of functional polymer materials with Si based PCRRs, which can lead to high speed modulators, suitable for photonic integration and RF photonics.

15. SUBJECT TERMS

Photonic crystals, ring resonators, silicon modulators, polymer photonics, RF photonics.

16. SECURITY CLASSIFICATION OF:			**17.LIMITATION OF ABSTRACT**	**18.NUMBER OF PAGES**	**19a. NAME OF RESPONSIBLE PERSON**
a. REPORT	**b. ABSTRACT**	**c. THIS PAGE**			Richard Soref
Unclassified	Unclassified	Unclassified	SAR	9	**19b. TELEPHONE NUMBER** *(include area code)* N/A

Standard Form 298 (Rev. 8-98)
Prescribed by ANSI Std. Z39.18

Ultra-Compact Polymer and Silicon Modulator Design Based on Photonic Crystal Ring Resonators

Zexuan Qiang[1], Weidong Zhou[1*], Richard A. Soref[2], and Zhenqiang Ma[3]
[1]*Department of Electrical Engineering, NanoFAB Center, University of Texas at Arlington, TX 76019, USA*
[2] *Sensors Directorate, Air Force Research Laboratory, AFRL/RYHC, Hanscom Air Force Base, MA 01731, USA*
[3]*Department of Electrical and Computer Engineering, University of Wisconsin-Madison, WI 53706, USA*

ABSTRACT

Ultra-small silicon-based photonic-crystal ring resonators (PCRRs), both passive and active, will be key contributors to the emerging low-power nanophotonic technology. We have modeled and simulated the diameter-dependent loss, Q, and FSR of such PCRRs and find a 0.02 dB "intrinsic" loss that is independent of diameter, unlike the ~1/D loss of micro-strip resonators. Close to 100% drop efficiency at the drop channel of 1557.5nm was obtained by design with a high spectral selectivity of Q greater than 1319 in the single-ring PCRR-based add-drop filters with ring radius of 1.2 μm. Ultra-compact polymer modulators were proposed and simulated, based on the hybrid integration of functional polymer materials with Si based PCRRs, which can lead to high speed modulators, suitable for photonic integration and RF photonics.

Keywords: Photonic crystals, ring resonators, silicon modulators, polymer photonics, RF photonics.

1. INTRODUCTION

There is an increasing and largely unfulfilled need for nanometer-scale photonic components, both passive and active, in intra-chip optical communications and other high-speed, ultra-low-power photonic applications. Some of the most compact microphotonic components developed for 1550-nm use, such as microring-resonator modulators [1-6], have a minimum useable diameter (D) of about 25 λ/n, where λ is the free-space wavelength and n is the refractive index of the silicon-on-insulator strip (or rib) waveguide from which the ring is made. For the nanophotonic "mission", it is desirable to scale D downwards in future versions of the device. However, the 1/D dependence of propagation loss in the microstrip [5, 7] presents a problem or "roadblock" to scaling [7]. Potentially, the photonic-crystal ring resonator (PCRR), which has a minimum D of around 5 λ/n, presents a solution to this problem-- if it can be shown that the PCRR insertion loss will be significantly lower than that of a micro- ring which has same diameter. This paper addresses the PCRR loss issue.

On the other hand, photonic crystals, offer great promise in ultra-compact photonic components. Photonic crystal add-drop filters (ADFs) have been reported with various defect and cavity configurations, with a single-defect cavity as the smallest resonators [8-13]. Recently we proposed and reported photonic-crystal ring resonators (PCRRs), with scalable ring sizes and flexible mode coupling configurations [14]. PCRRs can have a minimum D of around 5 λ/n. This may present a solution to the 1/D dependent loss problem-- if it can be shown that the PCRR insertion loss will be significantly lower than that of a micro- ring which has same diameter.

We first presents a detailed analysis of radiative waveguide bend loss in single-ring PCRR based add-drop filters (ADFs), as well as bend loss in micro-strip rings as a function of effective radius from 1 to 15 μm at λ ~ 1550 nm. The result is favorable: there is no significant size-dependent loss in the PC structures; in great contrast to the micro strip structures. A PC resonant cavity with 1 μm effective radius has an inherent total loss of 0.02 dB together with a modal Q factor of ~1300. In addition, the FSR of the PCRR can be tuned dramatically with radius.

We then presents a practical structure based on functional polymer and silicon dielectric rod PCRRs. Polymer-based modulators have attracted great attention due to their intrinsic high performance like low loss, low birefringence,

* wzhou@uta.edu.

high thermo-optic coefficient, environmental stability, high yields with easy processibility [15, 16]. There're two general structures to perform high-speed polymer modulators including Mach-Zehnder Interferometer (MZI) [17, 18] and micro-ring resonator [19-21] based structure. Traveling wave MZI polymer modulators require several mm ~ cm long optical path to achieve the desired phase shift, which brings phase matching problems to the RF design because the electrode length is comparable to RF wavelength. However in microring modulators, the electrode loss is not an issue and the bandwidth is set by the electrode capacitance since the device is small the electrode size can be much smaller than the modulation wavelength (even up to 100 GHz [22]) and the device's high-speed behavior is mainly capacitive. The hybrid integration of functional polymer materials with Si rods based PCRRs, can lead to ultra-compact, high speed modulators, suitable for photonic integration and RF photonics. We report here the simulated device characteristics with an effective ring radius of 2.3 μm and tunable polymer index from 1.785 to 1.805.

2. ESTIMATES OF SIZE DEPENDENT INSERTION LOSS IN SI RODS BASED PCRRS

The single ring optical add-drop filter (ADF) is schematically shown in **Fig. 1**(a), where the incident port and exit ports are labeled as A, B, C, D, respectively. The structure is based on the square lattice dielectric rods (n_h, 3.48) surrounded by the background of low index materials. The low index materials can be silica or polymer with index of 1.48-1.78, or simply air (n_l = 1). Comparable ADF performances can be obtained for both cases. Note that in **Fig. 1** (a) four additional dielectric-rod scatterers (blue color) with the same parameters (size and index) as all other dielectric rods were introduced to improve the spectral selectivity and drop efficiency [14]. The ratio of the rod radius r to the lattice constant a, is 0.185. Based on the simulated photonic dispersion curves, the photonic bandgap spans from 1270 to 1740 nm for lattice constant *a* of 540 nm.

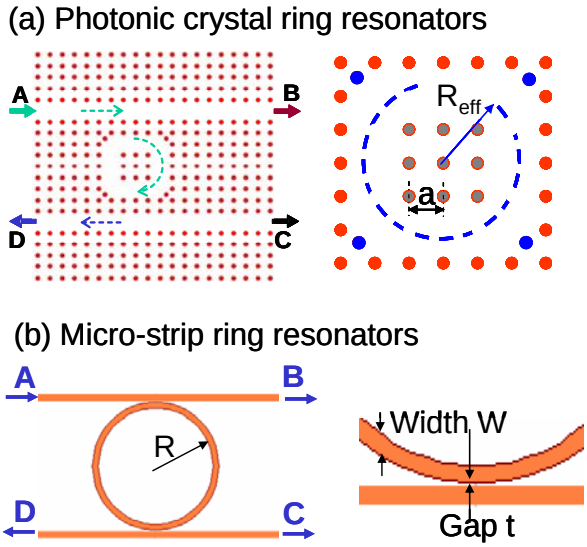

Fig. 1 (a) Schematic of photonic crystal ring resonators with effective radius R_{eff} defined as shown in the right plot; (b) Micro-strip ring resonators and the associated radius R.

We introduce an effective radius concept for PCRR structure based on equivalent area concept, as shown in Fig. 1 (a)(right), with $R_{eff} = (m+1)a/\sqrt{\pi}$, where m is the period of dielectric rods enclosed in the PCRR resonator (m = 3 for the structure shown). By changing the m values, the effective radius changes accordingly. For comparison, ADF based on micro-strip ring resonators, with similar configuration parameters, is used to simulate the transmission and loss properties, as shown in Fig. 1 (b), where the effective index is n_{eff} = 2.44, strip width and gap size are W = 500nm and t = 100nm, respectively. The lengths of the waveguide buses are kept the same for all cases in these two structures, which is L = 33.5 μm (or 62*a* for PCRR based ADFs). Ring radius R changes accordingly for size dependent loss analysis. Generally, there is a trade-off between the increase of the cavity Q and the decrease of the coupling/dropping efficiency [14]. The coupling strength, i.e., the number of coupling periods between the line defect waveguide bus and the PCRRs, was adjusted for high drop efficiency. The bus-ring coupling distance changed from two periods for small ring sizes

(e.g., the one shown in Fig. 1a), to three periods when the effective ring radius R_{eff} of PCRR increased to 2.44 μm and greater (with m>7).

The transmission characteristics were simulated with the two-dimensional finite-difference time-domain (FDTD) technique using perfectly matched layers (PML) as absorbing boundaries [14]. A Gaussian optical pulse, covering the whole frequency-range-of-interest, is launched at the input port A. Power monitors were placed at each of the other three ports (B, C, D) to collect the transmitted spectral power density after Fourier-transformation. All of the transmitted spectral power densities were normalized to the incident light spectral power density from input Port A. Simulations were carried out for Silicon PCRR and micro-strip ring resonator based ADFs. Shown in Fig. 2 (a) are the normalized transmission spectra for three output ports (B, C, D) in the single ring ADFs. Close to 100% drop efficiency at the drop channel of 1557.5nm was obtained with a high spectral selectivity of Q greater than 1319 in the single-ring PCRR-based ADFs, with effective ring radius R_{eff} of 1.2 μm. We determined that the spectral performance reported here is comparable to or better than that of the micro-strip ring resonators, as shown in Fig. 2 (b), with even large ring radius (R = 3 μm). The field patterns for the drop channels with different ring sizes for PCRRs and for the micro-strip ring resonators are also shown in Fig. 2 (right). The total normalized power at three output ports (B+C+D)/A is used to derive the total loss in the ADF devices, in units of dBs. It is worth mentioning that the total loss in the ADF devices derived here includes both the bending loss associated with small ring radius PCRRs as well as the coupling loss between the waveguide buses and the PCRRs.

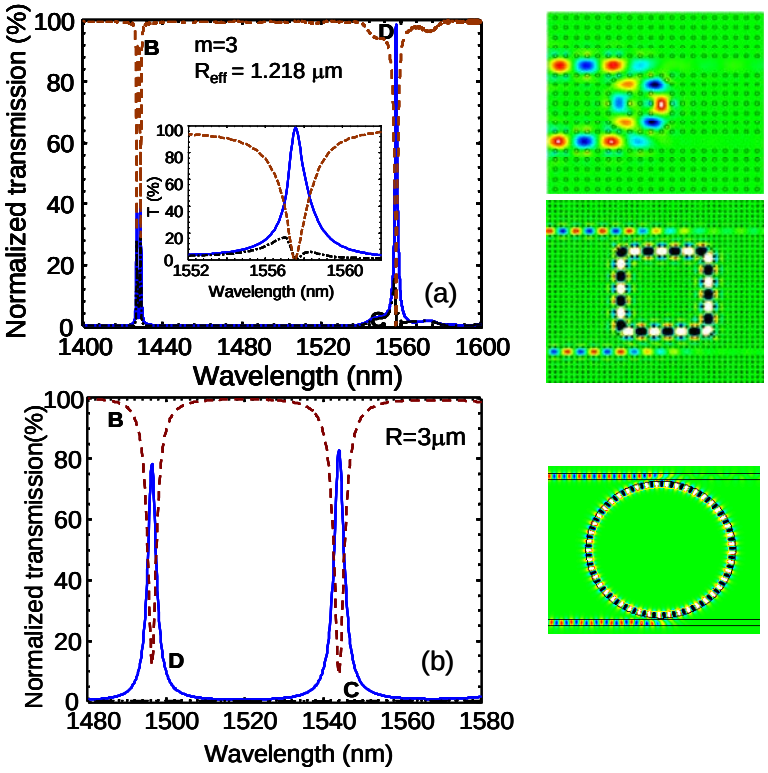

Fig. 2 Spectral response of single ring add-drop filters based on (a) PCRRs; (b) Micro-strip ring resonators. Shown to the right are the field patterns for the corresponding drop channels with different ring sizes.

The size dependent loss is shown in Fig. 3, for sing ring ADFs based on PCRR and for the corresponding micro-strip ring resonators. The lower portion of loss in PCRRs is shown in the inset of Fig. 3 (a zoom-in view). As expected, the bending loss increases drastically for ring radii less than 5μm in micro-strip ring resonators. On the other hand, we did not see any size dependent bending loss in PCRRs. We believe it is mainly due to the difference in the mode confinement mechanisms. The mode confinement in strip waveguide is provided by the total internal reflection (TIR) which leads to significant size dependent mode leakage as the bending radius reduces. In photonic crystal structures, the mode confinement is provided by the distributed coherent scattering and the photonic bandgap. When we assume that

the PC surface roughness is greatly minimized during PC fabrication, we find that the coherent scattering-and-bandgap give almost zero bending loss in PC waveguides that have bending angles of 90° and extremely small bending radii. When roughness is minimized, ultra-compact defect-mode cavities such as the ones reported here can be achieved in PCs and those cavities will have with extremely high Q and low volume.

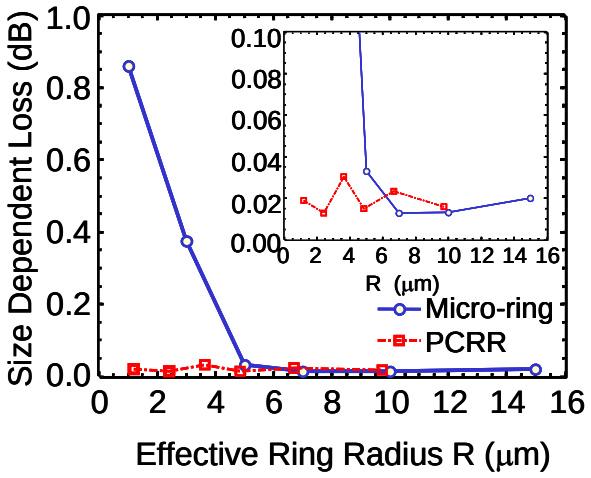

Fig. 3 Size dependent loss in PCRR and micro-strip ring resonator based ADFs. The low bend loss in PCRRs is shown in the inset.

The size dependent free-spectral range (FSR) values were investigated and compared for both PCRR and micro-strip ring resonators. One set of the data is plotted in Fig. 4 (a), which is derived from the simulated spectral response curves, as shown in Fig. 2, for different radii. It is interesting to note that the change in FSR associated with R_{eff} in PCRRs follows closely the FSR change for micro-strip based ring resonators. We tried to fit the data with theory. It is well known for micro-strip ring resonators that the relationship between FSR and ring radius R is[19]:

$$FSR(\Delta\lambda) = \frac{\lambda^2}{(n_{eff} - \lambda\frac{\partial n_{eff}}{\partial\lambda})\cdot 2\pi R} = \frac{\lambda^2}{n_g \cdot 2\pi R} \quad (1)$$

where λ is the resonant wavelength, n_{eff} and n_g are the effective index and group index of the ring, respectively. Assuming $n_g = n_{eff} = 2.44$ for the micro-strip ring resonators, the theoretical curve is plotted in Fig. 4(a), which agrees very well with the data from FDTD simulation.

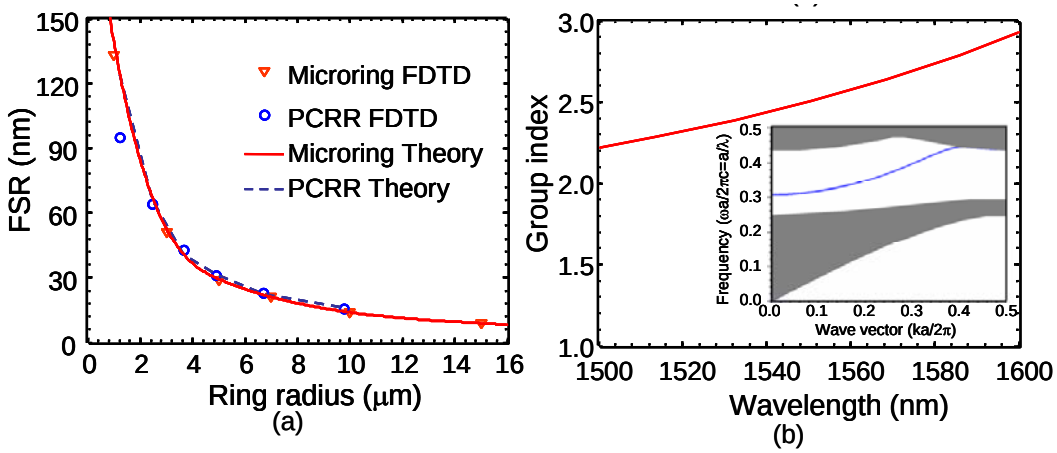

Fig. 4 (a) Size-dependent FSRs in micro-strip ring resonators and PCRRs based on FDTD simulation and theory; (b) Group index in PCRR structures based on the defect mode dispersion curve shown in the inset for the single line-defect bus-waveguide.

We attempted to use the same equation to find the relations between FSR and effective radius R_{eff} in PCRR structures. In addition, we can calculate the n_g from the photonic bandgap dispersion curve (frequency ω vs. momentum κ) with the equation: $n_g = c/v_g = c/(d\omega/dk)$, where c is the speed of light in vacuum, v_g is the group velocity and can be derived from the dispersion curve for the confined defect mode in the single-line-defect bus waveguide[23]. The n_g result is shown in Fig. 4 (b) for different R_{eff}. The dispersion plot for a single line-defect bus-waveguide is shown in the inset of Fig. 4 (b), which was simulated with the plane-wave expansion technique. Theoretical FSR values were calculated for each radius with different resonator wavelength and the corresponding group index based on Fig. 4 (b). As shown in Fig. 4 (a), very good agreement was obtained between theory and FDTD simulation for both structures.

3. PCRR POLYMER/SI MODULATORS

The functional polymer modulator with embedded Si rods PCRR add-drop filter configuration is shown in Fig. 5, where a disruptive silicon nanomembranes (SiNM) transfer process [24] is used to transfer the modulator structure onto the low index ITO coated glass substrate. The vertical waveguiding structure is the polymer filled Si rods PCRR core region sandwiched in between the low index polymer cladding layers. The device design parameters used in our design is also shown in Fig. 5. Electrical control is based on the bottom transparent ITO electrode and the top high speed electrode for high speed (RF frequency or greater than 100GHz). The ON/OFF modulator is done via free carrier injection/depletion induced index change, which leads to the resonance shift.

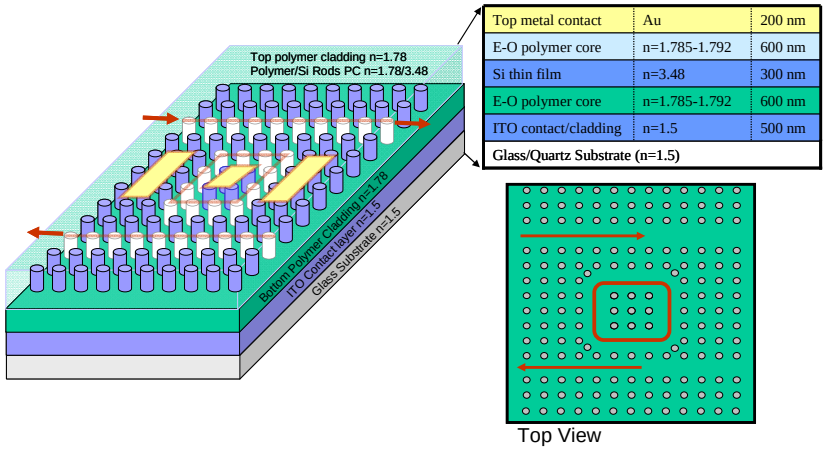

Fig. 5 Hybrid integration of functional polymers with Si PCRRs for RF photonic modulators with ultra-compact sizes: 3D, cross-sectional and top views of device structure based on Si PCRRs.

Using the aforementioned simulation technique, the normalized transmission characteristics were obtained for polymer based PCRR modulators composed of single line-defect (W1) PC waveguide and single ring PCRRs. The silicon index is 3.48, the Si dielectric rod radius r is 100nm, and the lattice constant of PC a is 379 nm. Note the effective radius of our PCRR is only 2.687 μm, which reduces the complexity of RF/microwave electrode design due to optic-microwave interaction region much less than the RF wavelength and thus can achieve high modulation speed. The optical channel signal propagating through W1 PC waveguide can be modulated by controlling the index of the coupled PCRR cavity region through electrical contact on top. At the *ON* state of the modulator, light confined by the photonic crystal structure travels along the W1 line defect waveguide, while at the *OFF* state, the PCRR ring defect is tuned to resonant at the working frequency and no light passes through the W1 waveguide.

Very high spectral selectivity can be achieved for different indices of polymers, as shown in Fig. 6. For an input signal of 1565.2nm, the modulation depth is about 25 dB with virtually 0dB insertion loss. The corresponding propagation field patterns are shown in the inset, for *ON* and *OFF* states. The drop channel wavelength changes from 1565.2 nm for polymer index of 1.785 (with zero bias voltage), to 1571.8nm for polymer index of 1.805 (with bias voltage of a few volts), as also shown in Fig. 7(a). The quality factor Q of the filter remains high for these different indices, with Q values greater than 10^5. Such high Q factors is easily achievable for different modes of resonators, as shown in Fig. 7(b), where the Q factors are all greater than 10^5 for three types of resonant modes.

These results illustrate the significant potentials associated with PCRRs, for ultra-compact ring resonators, for diffraction-limited photonic devices with high spectral selectivity, low switching/modulation power, and high modulation speed.

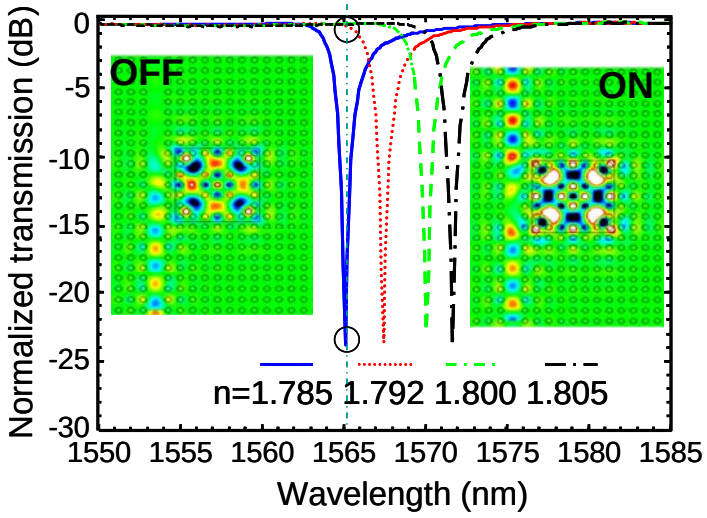

Fig. 6 Simulated spectral tuning characteristics for a single channel PC waveguide coupled with a single ring PCRRs embedded in an index tunable functional polymer material. The propagating field profiles for *ON* and *OFF* states are shown in the inset for the channel with center wavelength of 1565.2 nm at polymer indices of 1.805 and 1.785, respectively.

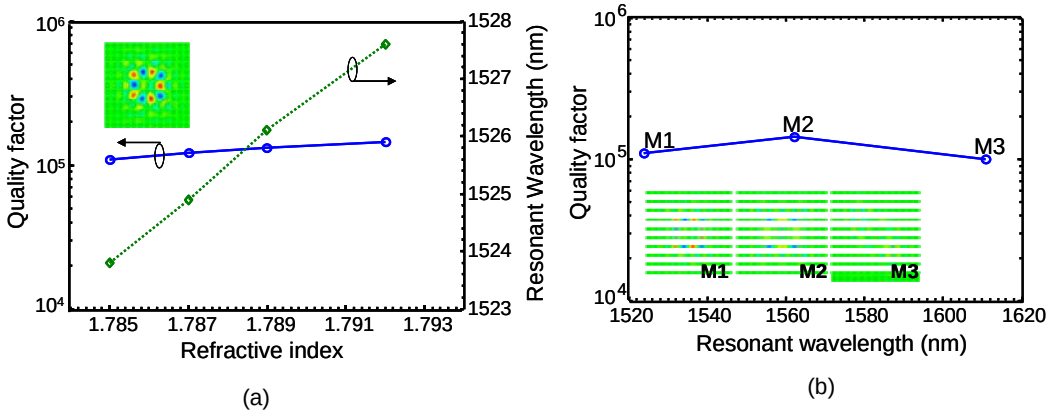

Fig. 7 (a) Top view of our Si/polymer PCRR modulator; (b) simulated modulation characteristics where the silicon index, polymer index, a and r/a are 3.48, 1.78, 0.379 μm, and 0.26, respectively.

4. CONCLUSIONS

In conclusion, we have investigated the properties of ultra-compact photonic crystal ring resonators. We prove there are no intrinsic size-dependent bending losses in PCRR-based structures. A high performance ADF was designed with effective ring radius of 1.2 μm, inherent total loss of 0.02 dB, drop efficiency close to 100%, and Q greater than 1,300. Using the dispersion-related group velocity, we also demonstrate that the free-spectral range in PCRRs has a similar dependence upon the effective ring radius as the one shown in micro-strip ring resonators. A practical modulator structure based on the integration of functional polymers with ultra-compact PCRRs was proposed and designed. Very high spectral selectivity is enabled with high cavity Q. Electrical control of polymer index can lead to high speed modulation. These findings make the PCRRs an alternative to current micro-ring resonators for ultra-compact WDM components and high density photonic integration.

5. ACKNOWDGEMENTS

The authors acknowledge the helpful discussions with Drs. Zhongyan Sheng and Y. Kevin Zou at Boson Applied Technologies, Inc. This work was supported in part by the U.S. Air Force Office of Scientific Research (Dr. Gernot Pomrenke).

References

[1] B. E. Little, S. T. Chu, H. A. Haus, J. Foresi, and J. P. Laine, "Microring resonator channel dropping filters," *IEEE J. Lightwave Technol.*, vol. 15, pp. 998-1005, 1997.

[2] Q. Xu, S. Manipatruni, B. Schmidt, J. Shakya, and M. Lipson, "12.5 Gbit/s carrier-injection-based silicon micro-ring silicon modulators," *Opt. Express*, vol. 15, pp. 430-436, 2007.

[3] M. Lipson, "Compact Electro-Optic Modulators on a Silicon Chip," *IEEE J. Select. Top. Quant. Electron.*, vol. 12, pp. 1520-1526, 2006.

[4] C. Manolatou and M. Lipson, "All-optical silicon modulators based on carrier injection by two-photon absorption," *IEEE J. Lightwave Technol.*, vol. 24, pp. 1433-1439, 2006.

[5] W. Bogaerts, D. Taillaert, B. Luyssaert, P. Dumon, J. Van Campenhout, P. Bienstman, D. Van Thourhout, R. Baets, V. Wiaux, and S. Beckx, "Basic structures for photonic integrated circuits in Silicon-on-insulator," *Opt. Express*, vol. 12, pp. 1583-1591, 2004.

[6] C. Li, L. Zhou, and A. W. Poon, "Silicon microring carrier-injection-based modulators/switches with tunable extinction ratios and OR-logic switching by using waveguide cross-coupling," *Opt. Express*, vol. 15, pp. 5069-5076, 2007.

[7] W. Zhou, Z. Qiang, and R. Soref, "Optical Add-Drop Filter Design Based on Photonic Crystal Ring Resonators," in *The Conference on Lasers and Electro-Optics (CLEO) 2007* Baltimore, MD, US: The Optical Society of America, 2007.

[8] S. Fan and J. D. Joannopoulos, "Analysis of guided resonances in photonic crystal slabs," *Phys. Rev. B*, vol. 65, p. 235112, 2002.

[9] M. Notomi, A. Shinya, S. Mitsugi, E. Kuramochi, and H. Y. Ryu, "Waveguides, resonators and their coupled elements in photonic crystal slabs," *Opt. Express*, vol. 12, pp. 1551-61, 2004.

[10] J. R. Vivas, D. N. Chigrin, A. V. a. Lavrinenko, and C. M. S. Torres, "Resonant add-drop filter based on a photonic quasicrystal," *Opt. Express*, vol. 13, pp. 826-35, 2005.

[11] Z. Zhang and M. Qiu, "Compact in-plane channel drop filter design using a single cavity with two degenerate modes in 2D photonic crystal slabs," *Opt. Express*, vol. 13, pp. 2596-2604, 2005.

[12] H. Takano, B. S. Song, T. Asano, and S. Noda, "Highly efficient in-plane channel drop filter in a two-dimensional heterophotonic crystal," *Appl. Phys. Lett.*, vol. 86, p. 241101, 2005.

[13] H. Takano, Y. Akahane, T. Asano, and S. Noda, "In-plane-type channel drop filter in a two-dimensional photonic crystal slab," *Appl. Phys. Lett.*, vol. 84, p. 2226, 2004.

[14] Z. Qiang, W. D. Zhou, and R. A. Soref, "Optical add-drop filters based on photonic crystal ring resonators," *Opt. Express*, vol. 15, pp. 1823-31, 2007.

[15] J. H. Burroughes and C. Jones, "New semiconductor device physics in polymer diodes and transistors," *Nature*, vol. 335, pp. 137-141, 1988.

[16] L. Eldada, "Polymer integrated optics: Promise vs. practicality," *Proc. SPIE*, vol. 4642, 2002.

[17] W. H. Steier, A. Chen, S. S. Lee, S. Garner, H. Zhang, V. Chuyanov, L. R. Dalton, F. Wang, A. S. Ren, and C. Zhang, "Polymer electro-optic devices for integrated optics," *Chem. Phys*, vol. 245, pp. 487-506, 1999.

[18] R. M. de Ridder, A. Driessen, E. Rikkers, P. V. Lambeck, and M. B. J. Diemeer, "Design and fabrication of electro-optic polymer modulators and switches," *Opt. Mat.*, vol. 12, pp. 205-214, 1999.

[19] P. Rabiei, W. H. Steier, C. Zhang, and L. R. Dalton, "Polymer Micro-Ring Filters and Modulators," *J. Lightwave. Technol.*, vol. 20, 2002.

[20] A. Leinse, M. B. J. Diemeer, A. Rousseau, and A. Driessen, "A novel high-speed polymeric EO Modulator based on a combination of a microring resonator and an MZI," *IEEE Photon. Technol. Lett.*, vol. 17, pp. 2074-2076, 2005.

[21] H. Tazawa, Y. H. Kuo, I. Dunayevskiy, J. Luo, A. K. Y. Jen, H. R. Fetterman, and W. H. Steier, "Ring Resonator-Based Electrooptic Polymer Traveling-Wave Modulator," *J. Lightwave Technol*, vol. 24, pp. 3514–3519, 2006.

[22] R. T. Chen, "Polymer-based photonic integrated circuits," *Opt. Laser Technol*, vol. 25, pp. 347–365, 1993.

[23] S.-H. Jeong, N. Yamamoto, J. Sugisaka, M. Okano, and K. Komori, "GaAs-based two-dimensional photonic crystal slab ring resonator consisting of a directional coupler and bent waveguides," *J. Opt. Soc. Am. B*, vol. 24, pp. 1951-9, 2007.

[24] H. C. Yuan, Z. Ma, M. M. Roberts, D. E. Savage, and M. G. Lagally, "High-speed strained-single-crystal-silicon thin-film transistors on flexible polymers," *J. Appl. Phys.*, vol. 100, p. 013708, 2006.